



THIS MANUSCRIPT HAS BEEN SUBMITTED TO THE ANNALS OF GLACIOLOGY AND HAS NOT BEEN PEER-REVIEWED.

Dye tracing of upward brine migration in snow

| | |
|-------------------------------|--|
| Journal: | <i>Annals of Glaciology</i> |
| Manuscript ID | Draft |
| Manuscript Type: | Article |
| Date Submitted by the Author: | n/a |
| Complete List of Authors: | Mallett, Robbie; Earth Observation Group, Department of Physics and Technology, UiT The Arctic University of Norway; University College London, Earth Sciences Stroeve, Julianne; University of Manitoba, Riddell Faculty Nandan, Vishnu; University of Manitoba, (2) Centre for Earth Observation Science (CEOS) Willatt, Rosemary; University College London, Earth Sciences Saha, Monojit; Centre for Earth Observation Science, University of Manitoba, CA Yackel, John ; University of Calgary, Geography Veyssiere, Gaelle; British Antarctic Survey Wilkinson, Jeremy; British Antarctic Survey, |
| Keywords: | Sea ice, Snow, Snow physics |
| Abstract: | The presence of salt in the snow overlying seasonal sea ice has profound thermodynamic and electromagnetic effects. However, the way that it arrives and is distributed within the marine snowpack remains poorly understood and modelled. We describe two experiments tracing upward brine movement in snow: one laboratory experiment at Rothera research station, West Antarctica, and a field experiment in Hudson Bay, Canada. The laboratory experiments involved the addition of dyed brine to the base of terrestrial snow samples, with subsequent wicking being characterised. After initial and total absorption at the base, the dyed brine migrated further up over nine days, ultimately reaching heights between 2.5 & 6 cm. Our field experiment involved dye being added directly (without brine) to bare sea ice and lake ice surfaces, with snow then accumulating on top over several days. On the sea ice, the dye migrated upwards into the snow by up to 5 cm as the snow's basal layer became more salty, whereas no dye migration occurred in our control experiment over lake ice. Upward dye migration and basal salinification over the sea ice occurred in relatively dry snowpacks where brine |

| | |
|--|--|
| | inclusions took up between 0.5 & 5.8% of the snow's pore volume. |
| | |

SCHOLARONE™
Manuscripts

Dye tracing of upward brine migration in snow

Robbie MALLETT,^{1,2,†} Vishnu NANDAN,^{3,4,5,†} Julienne STROEVE,^{2,3,6} Rosemary WILLATT,^{7,2}
Monojit SAHA,³ John YACKEL,⁴ Gaëlle VEYSIÈRE^{2,8} Jeremy WILKINSON⁸

[†] *These authors contributed equally to this work*

¹*Earth Observation Group, Department of Physics and Technology,
UiT The Arctic University of Norway, Norway*

²*Centre for Polar Observation and Modelling, Department of Earth Sciences,
University College London, UK*

³*Centre for Earth Observation Science, University of Manitoba, Winnipeg, Canada*

⁴*Cryosphere Climate Research, Group, Department of Geography,
University of Calgary, Canada*

⁵*H2O Geomatics Inc, Kitchener, Ontario, Canada*

⁶*National Snow and Ice Data Center,*

University of Colorado, Boulder, CO, USA

⁷*Centre for Polar Observation and Modelling, Department of Geography
and Environmental Sciences, University of Northumbria, UK*

⁸*British Antarctic Survey, Cambridge, UK*

Correspondence: Robbie Mallett <robbiemallett@gmail.com>

ABSTRACT.

The presence of salt in the snow overlying seasonal sea ice has profound thermodynamic and electromagnetic effects. However, the source and pathways through which it arrives and is distributed within the marine snowpack remain poorly understood and modelled. Here we describe two experiments tracing upward brine movement in snow: one laboratory based experiment at Rothera research station, West Antarctica, and a field-based experiment in Hudson Bay, Canada. The laboratory experiments involved the addition of dyed brine to the base of terrestrial snow samples, with subsequent wicking being characterised. After initial and total absorption at the base through

29 capillary action, the dyed brine migrated further up over nine days, ultimately
30 reaching heights between 2.5 & 6 cm. We attribute this further upward mi-
31 gration over time to gradual microstructural reconfiguration of the snow and
32 dilution of the brine from internal melting. Some dyed brine was eventually
33 released from the base of the sample into the container, potentially also due to
34 these processes. The height to which the brine was wicked was strongly related
35 to the bulk basal salinity of the samples and the salinity of the brine that was
36 later released. However, despite the temperature of the experiment remaining
37 consistent throughout, it was not clearly related to measured snow geophysical
38 properties such as density and specific surface area. This indicates that other
39 uncharacterised variables, such as pore connectivity, may principally control
40 the wicking height in our experiment. However, other evidence suggests that
41 the samples were equilibrating at different rates and some had not fully done
42 so after nine days. Our field experiment involved dye being added directly
43 (without brine) to sea ice and lake ice surfaces, with snow then accumulating
44 on top over several days. On the sea ice, the dye migrated upwards into the
45 snow by up to 5 cm as the snow's basal layer became more salty, whereas no
46 dye migration occurred in our control experiment over lake ice. Upward dye
47 migration and basal salinification over the sea ice occurred in relatively dry
48 snowpacks where brine inclusions took up between 0.5 & 5.8% of the snow's
49 pore volume.

50 INTRODUCTION

51 Sea ice in both polar regions is becoming increasingly seasonal due to the decreasing area of sea ice which
52 survives each summer melt season (Stroeve and Notz, 2018; Babb and others, 2023). The snow on the
53 increasing fraction of first-year ice (FYI) is geophysically distinct from that on the decreasing fraction
54 of multi-year ice because of its characteristic salinity. Snow salinity on FYI can reach upwards of ten
55 parts per thousand in the basal snow layers (Nandan and others, 2017). The presence of such a quantity
56 of salt modifies the thermodynamic and electromagnetic properties of the snow, which in turn affect its

57 geophysical evolution (e.g. Crocker, 1984). Alteration of the snow's dielectric properties impact active and
58 passive microwave remote sensing (Barber and others, 1998; Nandan and others, 2020).

59 Despite its importance, the source and pathways that deliver salt into the snow are still poorly under-
60 stood; potential mechanisms range from deposition of salt-aerosols from nearby open water areas, wind-
61 driven redistribution of snow grains that have saltated over newly formed sea ice, and upward capillary
62 action from newly-forming ice (Perovich and Richter-Menge, 1994; Dominé and others, 2004). This com-
63 plexity has so far prevented Arctic Ocean snow models such as SnowModel-LG (Liston and others, 2020)
64 and NESOSIM (Petty and others, 2018) from including salt-related processes in their modeled snowpacks.
65 Wever and others (2020) recently adapted the one-dimensional SNOWPACK snow model for the sea ice
66 environment. It is now capable of simulating flooding of the snow from negative ice freeboard, and has a
67 sophisticated scheme for handling downward percolation of water based on its parameterization of snow
68 microstructure. However, it has not yet clearly exhibited upward movement of brine into the snow from
69 capillary pressure, or reproduced the typical vertical profiles of snow salinity observed in-situ. If any of
70 the models mentioned above are to accurately reproduce these profiles then the real-world processes that
71 produce them must first be characterised. Here we use dye-tracing for tracking the upward movement of
72 brine in both the laboratory and field-based experiments.

73 **The nature and importance of snow salinity**

74 Fresh (used here to mean non-saline) snow has a melting point of 0°C. While microscopic quasi-liquid
75 layers do exist on the surface of snow grains below that temperature (Sazaki and others, 2012), a fresh
76 snowpack does not exhibit liquid water in quantities relevant to most thermodynamic or electromagnetic
77 considerations below 0°C. When salt is introduced to the snowpack in limited quantities, the physics of
78 the system is changed from a two-phase (air/ice) system to a three-phase system (air/ice/brine), and this
79 excludes the complication of salt precipitating out of the brine to create a fourth mixture component
80 (see Butler and others, 2016, for this precipitation in sea ice itself). Put simply, the presence of salt in
81 snow allows saline liquid water (brine) to coexist in a phase equilibrium with the ice lattice at sub-zero
82 temperatures (Stogryn, 1986; Geldsetzer and others, 2009).

83 Water is an excellent conductor of heat relative to ice and air, and so the thermal conductivity of
84 the ice/air/water mixture is increased (Crocker, 1984). Furthermore, water is an excellent absorber of
85 microwaves relative to ice and air (Drinkwater and Crocker, 1988); this reduces the ability of microwaves to

Mallett and others:

86 penetrate the saline snowpack on FYI. This effects coherent microwaves transmitted from and backscattered
87 to radars such as altimeters and scatterometers (Barber and Nghiem, 1999; Nandan and others, 2016, 2017;
88 Yackel and others, 2019; Nandan and others, 2020), but also natural microwave emission from the snow-
89 covered ice surface as measured by radiometers (e.g. Barber and others, 1998, 2003; Markus and others,
90 2009).

91 The presence of salt within snow-covered sea ice also affects the lower atmosphere. As well as being
92 photochemically relevant (Dominé and Shepson, 2002; Wren and others, 2013), saline snow produces salt
93 aerosols when redistributed by wind (Frey and others, 2020; Confer and others, 2023). This can nucleate
94 clouds, in turn modifying the radiative balance of the atmospheric boundary layer (Gong and others, 2023).

95 **Potential mechanisms for production of saline snow over first-year ice**

96 The processes that dictate the timing and extent of snow salinification over sea ice are not well understood
97 (Dominé and others, 2004). This is in part because the snow cover on sea ice is frequently redistributed by
98 the wind, making a single vertical column of snow (like that represented by a 1-D model such as Wever and
99 others (2020)) both difficult to observe continuously and often not representative of heavily redistributed
100 snow on an ice floe.

101 Dominé and others (2004) discuss three main potential mechanisms of salinification: deposition from
102 above by either (1) wind-blown frost flowers, (2) sea salt aerosol generated by sea spray, or (3) transport
103 from the ice below via capillary forces. Here, we focus on the contribution from the latter mechanism of
104 upward wicking via capillary action, and this requires the presence of brine at the base of the snowpack.
105 There are two typical routes that deliver brine to this location. One involves the presence of a thin layer of
106 brine that is deposited on the sea ice surface during its formation, described as a brine *skim* by Perovich
107 and Richter-Menge (1994). This might be upwardly rejected during nilas formation or the consolidation
108 of frazil ice, or might be left on the ice surface having spilled over the side of a piece of pancake ice due
109 to wave action. While the skim may mostly freeze as the ice thickens and its upper surface cools, falling
110 snow will increase the skim's volume by providing thermal insulation from the cold air. If it has sufficient
111 volume, brine from the skim can then potentially migrate upwards in the snow via capillary action. In this
112 case, moisture is scarce, and we suggest the height of wicking will likely be limited by the brine supply
113 simply running out.

114 Another mode of brine delivery to the base of the snowpack is flooding of the ice surface (e.g. Provost

115 and others, 2017). This occurs when so much snow accumulates that it presses the ice below the waterline.
116 In this case, the brine supply is often abundant, and the height of subsequent wicking will likely be limited
117 by the ability of the snow microstructure to sustain the surface tension required to hold the liquid up
118 against gravity. A photo of the phenomenon is given in Figure 2 of Willatt and others (2010), and we also
119 include a higher resolution colour photo of the phenomenon in Supplementary Figure S1. This phenomenon
120 was visualised by Massom and others (2001, see their Figure 6) by introducing dyed brine to the base of
121 an Antarctic snow sample and photographing the result shortly afterwards.

122 Here, we present a series of experiments following Massom and others (2001) which investigate the
123 potential of coloured dye to trace the upwards migration of brine both instantaneously and over time. We
124 begin by detailing laboratory based investigations where dyed brine is introduced at the base of terrestrial
125 snow samples, and the brine transport is visibly traced upwards. By introducing brine, we mimic flooding
126 of the base of the snow and subsequent wicking above the waterline. We then show how this technique can
127 also be used in a real sea ice environment with a positive freeboard: we show results of a pilot study on
128 landfast FYI and lake ice in Hudson Bay, Canada. In this case, we suggest the wicking can be attributed
129 to what remains of a brine skim. Finally, we reflect on the shortcomings of both experiments, and make
130 suggestions for future research directions.

131 METHODS

132 Dye Selection

133 We use a Rhodamine-WT dye to trace the migration of brine from the snow/sea ice interface. This
134 fluorescent, pink dye has a freezing point of 0°C and a specific gravity of 1020 kgm⁻³ (at 25°C). Compared
135 to other water tracing dyes, it has a relatively low cost and has a low minimum detectability (Smart and
136 Laidlaw, 1977; Davis and Dozier, 1984). It also has the advantage of having a similar density to brine, and
137 having the same freezing point as pure water. The latter characteristic means that where salt does not
138 exist, the dye will not alter the properties of the water itself, nor melt snow in areas where no liquid exists.
139 We manually verified that the addition of the dye to water does not alter its conductivity as measured by
140 an Oakton CON 450 conductivity meter, which was used for all field-based salinity analysis.

141 At this point we point out four other studies that have used tracer dyes to study *downward* liquid
142 movement in the sea ice context, in addition to Massom and others (2001) which was mentioned in our
143 introduction. Nicolaus and others (2009) used Sulforhodamin-B (SB) to trace the downward percolation

144 of snow meltwater in the spring-summer transition in the Weddell Sea. We elected not to use SB due to
145 its hydrophilic properties, which were raised by the authors in their study. SB was also used alongside
146 fluorescein by Freitag and Eicken (2003) to study sea ice permeability to meltwater, following Eide and
147 Martin (1975) who used thymol-blue and Bennington (1967) who used a proprietary dye named Dy-Chek
148 designed for automobile inspections.

149 **Rothera Laboratory Experiments**

150 We performed two rounds of laboratory experiments each lasting nine days at Rothera research station in
151 West Antarctica during August and October 2023. In each round, we identified two distinct stratigraphic
152 layers in nearby terrestrial snow that would allow us to take ten similar snow samples from each layer.
153 We produced 20 labelled polyvinylchloride (PVC) tubes (19 cm long, 6.4 cm internal diameter) which
154 could be driven into our chosen snow layers horizontally, and then extracted with a snow sample inside
155 (Figure 1a). This allowed us to extract several internally homogenous cylindrical snow samples of similar
156 snow properties upon which we could experiment. We first cooled the plastic tubes in nearby snow before
157 inserting them into the layers such that their temperature matched the samples as the tubes were driven
158 in. While establishing our protocol, we found that not cooling the tubes led to the snow sample adhering
159 to the sides and behaving erratically during the experiment.

160 After the samples were extracted from their respective layers, we took manual density measurements
161 of the layers using a 250 cm³ cylindrical snow cutter with a 5 cm internal diameter. We also separately
162 measured the layers in-situ with a snow micropenetrometer (v4 Schneebeli and Johnson, 1998) to estimate
163 the density and specific surface area of the snow using the method and coefficients of Proksch and others
164 (2015a).

165 Once the snow samples were brought into the lab, they were left in the freezer at $\sim -5.6^{\circ}\text{C}$ for at least
166 one hour. This allowed them to come to a common temperature with each other before having brine added,
167 but also produced a consistency of treatment between rounds. Because of its gas-based thermostat, the
168 freezer that hosted our experiments underwent thermal cycling where the compressor would periodically
169 switch on and off. To investigate the impact of such a cycle, we created a dummy sample where a digital
170 temperature logger was encased in snow during the second round of the experiments in October. The logged
171 temperatures are shown in Supplementary Figure S2, and had a mean value of -5.61°C and a standard
172 deviation of 0.22°C in the nine-day period for which the dummy sample was present in the freezer alongside

173 the main experiment.

174 Samples were seated in 100 ml plastic weighing boats, visible in white at the base of the sample in
175 figure 1b. This allowed the same amount of brine to be consistently supplied to the base of each sample.
176 Earlier attempts at the experiments saw several samples seated in the same tray, and brine added to the
177 tray (Supplementary Figure S3). Because of small inconsistencies in the sample extraction procedure or
178 the cutting of the plastic tubes, the ‘one tray’ approach led to some samples taking up the brine faster than
179 others, leading to inconsistent handling of different samples within the same round. In the final iteration
180 of our experiments (presented here), 50 ml of brine was added rapidly to each sample successively. We
181 discuss the salinity of the brine below. Samples took up all the brine within a few seconds; we provide a
182 video (Supplementary Video S1) of this immediate uptake using a special setup where the PVC tube is
183 suspended with a clamp stand to improve visibility.

184 To make our experiments as easy to interpret as possible, we chilled the dyed brine to the temperature
185 of the snow by storing it in the freezer where the snow samples equilibrated. Adding the brine at the
186 temperature of the snow ensured that there was no exchange of sensible heat between the brine and the
187 snow upon addition. The decision to do this influenced our choice of brine salinity: the brine must reliably
188 not freeze while in storage (even partially), but it also must not be so saline that salt would precipitate
189 out in storage. For example, using simple dyed seawater would have resulted in the formation of sea ice
190 at the temperature of the freezer, but five hundred parts of salt added to a thousand parts water would
191 not dissolve completely. To ensure we selected an appropriate salinity, we considered the phase function of
192 seawater brine near its freezing point (Figure 1 of Weeks, 1968). Following Equation 1c from Frankenstein
193 and Garner (1967), the equilibrium brine salinity (S_b) at a given temperature (T) can be described:

$$S_b = \frac{T}{T - 54.11} \quad (1)$$

194 Our dummy sample indicated that the freezer was operating at a mean temperature -5.61°C , with a
195 corresponding equilibrium salinity (S_b) of 94 ppt. We therefore selected a brine salinity of 100 ppt to ensure
196 that there would be no partial freezing of the brine in storage.

197 Because of the way the tubes were inserted into the snow layers, the snow adjacent to the plastic likely
198 experienced friction and compression. This led to edge-effects which meant it was not possible to observe
199 the height of internal brine wicking by looking at the snow sample from the outside, even when the plastic
200 tube was removed. Samples therefore had to be dissected with a snow scraper and viewed in cross-section

Mallett and others:

201 for the wicking height to be reliably established. Figure 1c shows a sample's dissected cross section, as well
202 as the edge effects that run vertically up the sides of the samples.

203 Once dissected, the sample's cross-section was photographed alongside a ruler. The camera was placed
204 at a consistent distance from the samples such that photos are intercomparable. The height to which the
205 snow was dyed was not always horizontally consistent. To generate a single, indicative height value for
206 inter-comparison between samples, the maximum and minimum wicked height in a sample were horizontally
207 referenced to the ruler (to the nearest millimetre, and then averaged. The height of wicking at the sample
208 edges was not considered when characterising the maximum height due to the edge effects discussed above.

209 Two stratigraphic layers were sampled in each round, with the two rounds of sampling occurring on
210 the 21st of August and the 5th of October. We had 20 sampling tubes, so allocated ten to each layer in
211 each round (thus sampling four layers over the two rounds). For each round, we sampled what at the time
212 were subjectively observed to be a hard snow layer and a soft snow layer. Henceforth, these layers will
213 be referred to as August Soft, August Hard, October Soft and October Hard. After the addition of dyed
214 brine, eight of the ten samples from a layer were placed in the freezer. In round one, the remaining two
215 samples from each layer were immediately dissected and the initial wicking height was characterised - they
216 were found to be similar. This similarity led to only one sample being immediately dissected in round two.
217 This made an additional snow sample available for each of the layers in round two, which we elected to
218 not add brine to. Instead we monitored the degree to which the sample settled in the tube in the absence
219 of brine addition, for later comparison with the measured sinking of the samples with brine in them. A
220 schematic of the sample allocation is given in Supplementary Figure S4.

221 By the end of the nine day experiment, the samples to which brine had been added had settled sig-
222 nificantly in their tubes, and had released dyed brine back out into the weighing boat, which began to
223 freeze over by the end of the experiment. This is visible in Figure 1b: the snow originally filled the black
224 tube to the top, and a halo of pink released brine has appeared around the bottom of the tube in the
225 weighing boat. The partially-frozen released brine was weighed, brought to room temperature, and its
226 salinity then was measured. Because the distance by which the snow surface had sunk could be measured
227 non-destructively, this was recorded every day. When each sample was eventually dissected and the wicking
228 height was measured, the salinity of its bottommost 3 cm layers was also recorded (0-3 cm, 3-6 cm). All
229 salinity measurements were taken using a Thermo Scientific Orion Star A221.

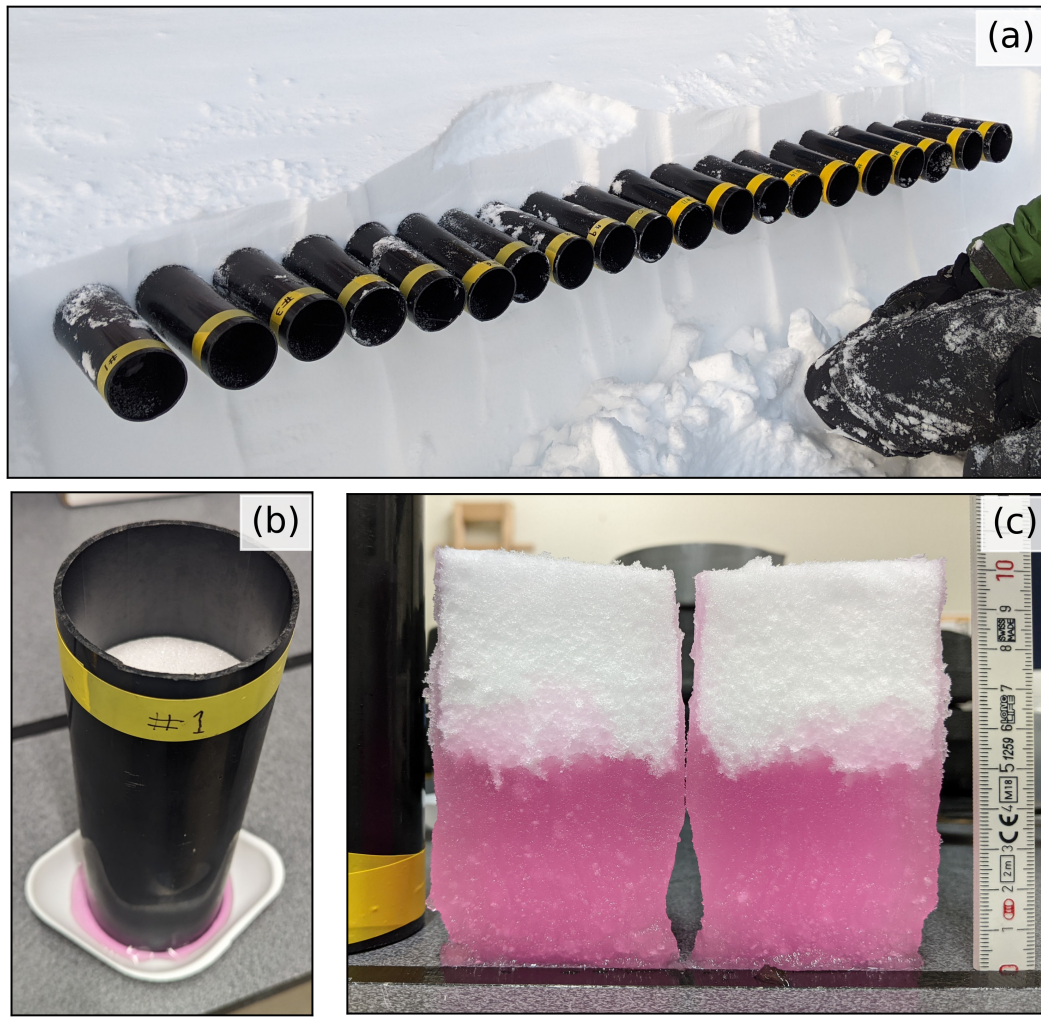


Fig. 1. Photographs showing the experimental procedure. (a) 19 cm plastic tubes were driven into a coherent layer of snow such that they each contained a sample with similar snow properties. In this photo the tubes are protruding from the wall of the snow pit. To sample the snow, they were pushed all the way in and then dug out by hand. (b) Snow samples were then taken to the laboratory, where they were brought to a consistent temperature and then dyed brine was added to the base. Photograph shows the sample after several days: the snow surface has sank within the tube, and the sample has begun to reject some brine back into the weighing boat. (c) At the end of the experiment, samples were removed from the tubes, dissected and photographed against a ruler. Geophysical sampling was then performed on the sample.

230 Churchill Field Experiments

231 Our field study was performed on newly-formed sea and lake ice near Churchill in the Western Hudson Bay
232 of Canada during December 2021. By the time we were able to get onto the sea ice with the dye, a thin
233 snow cover of ~ 5 cm had already accumulated. This posed the problem of how the dye could be supplied
234 to the base of the snowpack. We cleared a patch of sea ice by gently clearing the snow using a shovel and
235 then a stiff-bristled brush, aiming to minimally disturb the ice surface. We then applied the dye to the ice
236 surface in its neat form, without mixing it with brine as in the lab experiments. We then hypothesised that
237 the subsequent snow accumulation (from fresh snowfall and blowing snow) would insulate the ice surface,
238 such that a liquid phase would emerge, mix with the dye, and wick up into the snow.

239 At the first site on the 4th December (Dye Pit 1; DP1) we applied the dye directly from the bottle in
240 a line on the ice surface (Figure 2a). This was to help characterise lateral migration of the dye, as well as
241 vertical. At the second (DP2; ~ 10 m away) on the 9th December, it was sprayed over an area approximately
242 0.3×1 m from a spray bottle (Figure 2b). This was motivated by more even dye application, with the
243 potential to better characterise the horizontal variability of the vertical brine migration - unfortunately
244 this did not transpire and the spray-gun gave a somewhat patchy application. After dyeing the ice surfaces,
245 snow was allowed to accumulate over several days. The sites were then revisited throughout the campaign
246 (see Figure 2c for timeline), with a snow pit dug at each site at each visit (DP1 & DP2).

247 We also set up a control experiment (Control Pit; CP) on nearby lake ice, with dye applied via spray-
248 gun in a similar fashion to DP2 on the sea ice. The dye was applied on the 9th December, on the same day
249 as DP2. This control experiment was designed to show that the dye does not possess some inherent wicking
250 property independent of brine migration. If the dye at CP was seen to migrate up the snow without the
251 presence of salt, then it would invalidate the dye as an experimental tool for monitoring brine dynamics.
252 The control experiment was performed on a frozen lake 4.7 km south of the sea ice sites DP1 & DP2.
253 At the time of the dye application, the lake ice thickness was 58 cm. At both the beginning and the end
254 of the experiment snow and ice salinities were measured to be < 0.02 ppt. This is more than an order of
255 magnitude smaller than the lowest salinity recorded at the sea ice sites, and approaching the resolution
256 of the salinity meter stated by the manufacturer (0.01 ppt; Industrial Process Measurement Inc., 2016).
257 Supplementary Figure S5 shows the relative locations of the field sites.

258 Prior to applying the dye, we took scrapings of the ice surface to characterise its salinity. When we
259 revisited the sites to measure the dye migration and dig snow pits, we measured the ice surface salinity,

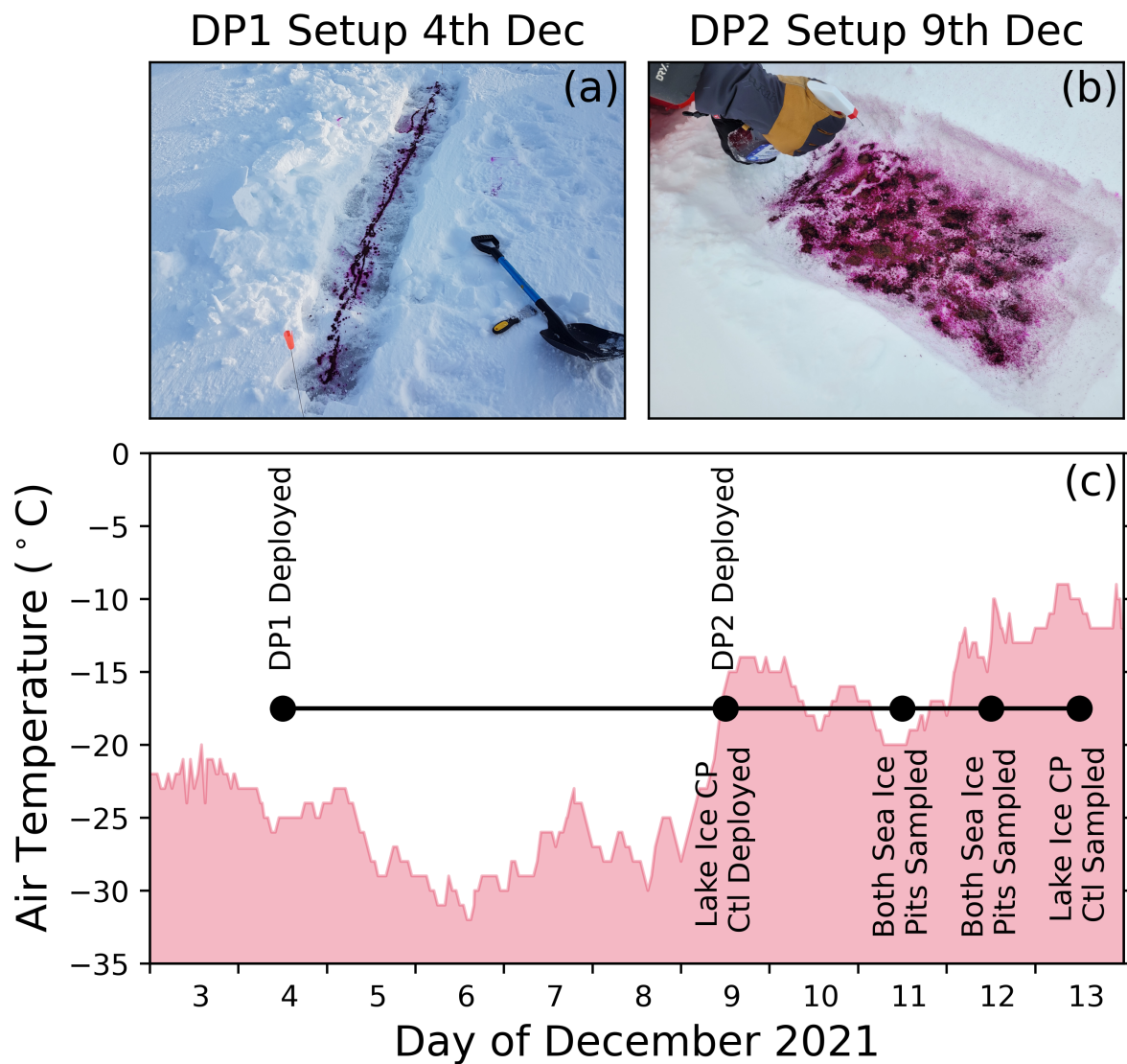


Fig. 2. (a) The setup of DP1, where dye was applied ‘neat’ from the bottle in a line onto the sea ice surface after snow clearing. This was to help characterise horizontal migration. (b) Setup of DP2, where dye was more evenly applied over an area with a spray bottle. (c) Timeline of the deployment and sampling of the three sites described in this manuscript: DP1, DP2, CP. The red-shaded timeseries indicates the air temperature recorded hourly at the Churchill airport 15.5 km to the west-south-west of the sea ice sites. Air temperatures measured at the airport were consistently below -10°C for the duration of the sea ice experiment.

260 and the snow density, temperature, and salinity at 2 cm vertical intervals. We measured the height of dye
261 migration with a ruler, and took photographs. At DP1, where the dye was applied in a line (Figure 2a),
262 we measured the dye migration height directly above the line along which the dye was applied (Figure 7a,
263 b & c). For DP2 (where the dye was distributed with a spray-gun, Figure 2b), we took the average of
264 the minimum and maximum height to which the dye had migrated over the region in which it was applied
265 (Figure 7d & e), similar to the laboratory measurement protocol. We note that the dye migration height
266 was recorded in the field, rather than extracted from the photos shown in Figure 7. Snow density was
267 measured with a 66 cm³ density cutter which allowed layer-wise sampling with a vertical resolution of 2
268 cm.

269 RESULTS

270 Rothera Laboratory Experiments

271 The snow micropenetrometer measurements indicated that the hard and the soft layers sampled in both
272 August and October were geophysically distinct with regard to retrieved density and specific surface area
273 (SSA; Figure 3). The soft snow sampled in October had properties that departed the most from the other
274 three, both in terms of density and SSA. The SMP's density retrievals consistently overestimated that
275 which we measured with our 250 cc density cutter. We note that evidence from Proksch and others (2016)
276 indicates that the cylindrical cutter itself may overestimate snow densities relative to micro-CT derived
277 estimates.

278 In Figure 3 we only show data from the first 30 mm of probe penetration, despite collecting data over a
279 relatively large probe penetration range. This is because snow in the upper levels of the layers was removed,
280 so as to be certain that the first snow encountered by the probe was from the layer that provided the snow
281 samples to the brine wicking experiment. So while the first few centimetres of SMP data are consistently
282 reliable, the probe in some cases then encountered the layer below which was not sampled and so is not
283 relevant to our investigation and not shown here.

284 All four of the snow layers samples immediately soaked up all the 50 ml of 100 ppt brine that was applied
285 (see Supplementary Video 1). In our first experimental round, we immediately dissected two samples from
286 each of the two layers. Their cross-sections revealed that the brine had wicked to a height of around 3.5
287 cm for both the hard and the soft snow. In the second round, we incorporated two control samples where
288 brine was not added, so only cut one sample from each layer open initially. The heights were 2.2 cm for

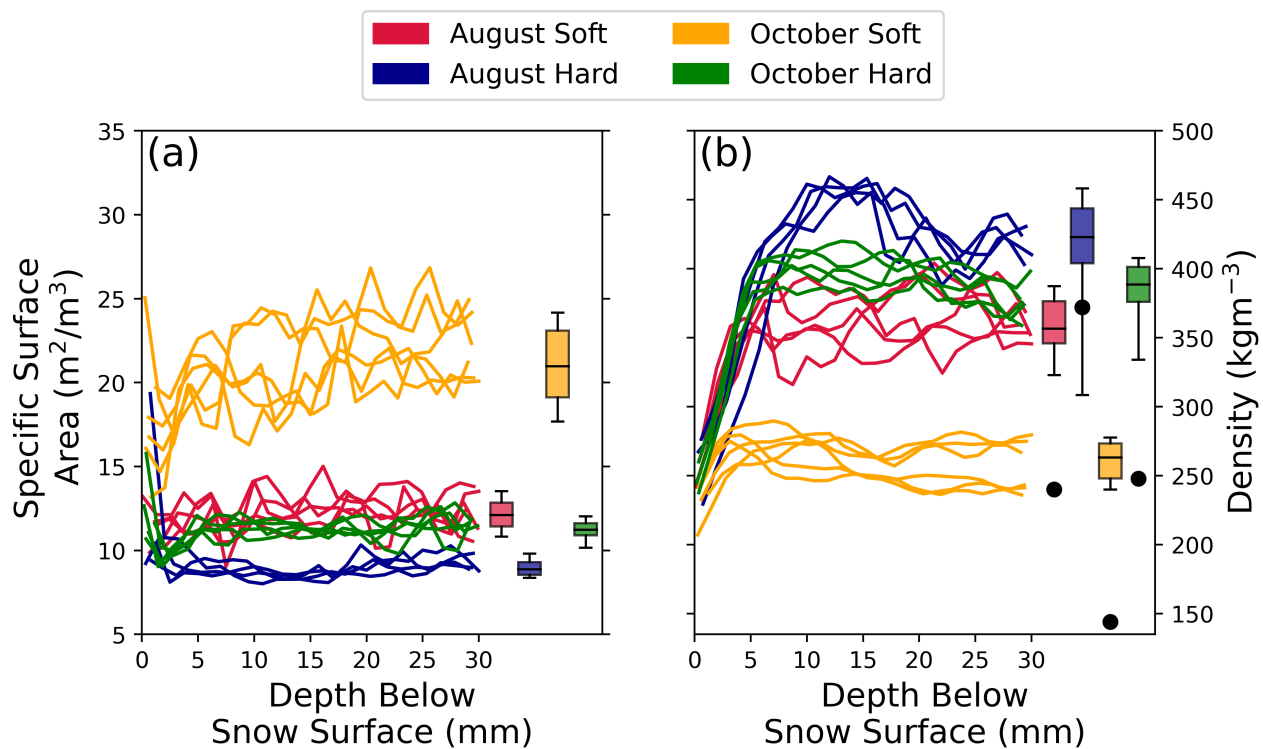


Fig. 3. (a) Specific surface area and (b) density from the four snow layers sampled over the first 30 mm of probe penetration. Line plots indicate the SSA/density retrievals based on the parameterization of (Proksch and others, 2015b). Box plots indicate the distribution of data from all five samples of each layer over the 30 mm range. Whiskers of the box plots indicate the 10th and 90th percentile, horizontal central lines indicate means. Round markers in panel (b) indicate the mean of the three manual density measurements performed on each layer with the 250 cc cylinder.

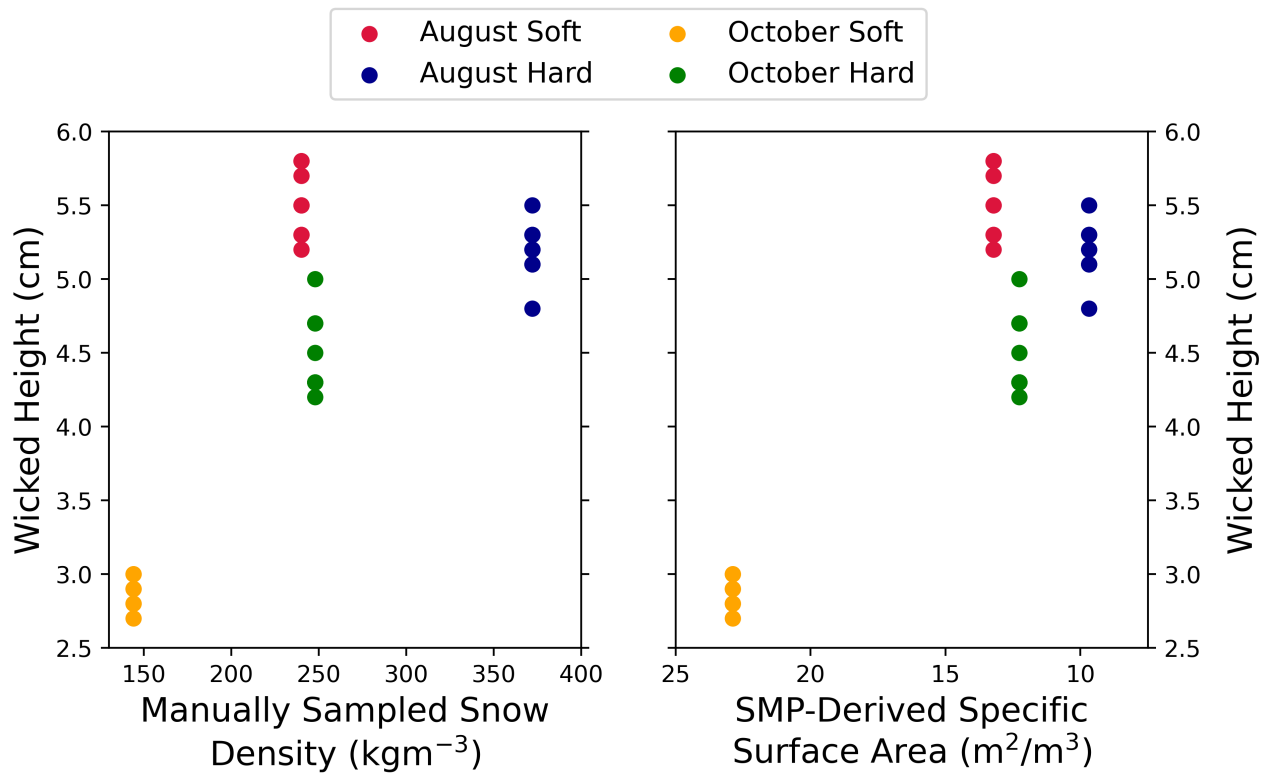


Fig. 4. Height to which dyed brine wicked in snow samples, shown as a function of snow density and estimated specific surface area. Samples displayed with a single x-coordinate based on the mean of in-situ measurements of the snow layer from which they were taken.

289 both the hard and the soft snow.

290 After waiting nine days, the height to which dye was present increased across all four snow layers. As
 291 a percent of the initial height reached, the 10-day heights were 153%, 150%, 131% & 204% for samples 1 -
 292 4 respectively (5.5, 5.2, 2.9, 4.5 cm total height, on average). A clear relationship between wicking heights
 293 and the density/SSA measurements is not evident (Figure 4). However, it is clear that the sample with
 294 the lowest density (and highest SSA) did wick substantially less than the other samples.

295 While the dye ascended into the snow samples over time, it also appeared to be a much less vivid shade
 296 of pink. This is consistent with significant dilution of the dyed brine solution. We validated this with
 297 bulk salinity measurements of the samples' bottom 3 cm. The bottom 3 cm of layers 1 - 4 exhibited the
 298 following initial bulk salinity values: 61.3, 61.2, 58.5, & 67.1 ppt. After 10 days, the average bulk salinity
 299 in the same 0 - 3 cm section of the samples was depleted to average values of 28.9, 35.7, 47.5 & 38.1 ppt.
 300 The basal bulk salinity of the samples was inversely correlated with the height to which the dye wicked
 301 (Figure 5b; $r = 0.92$, slope = -6.1 ppt per cm of wicked height).

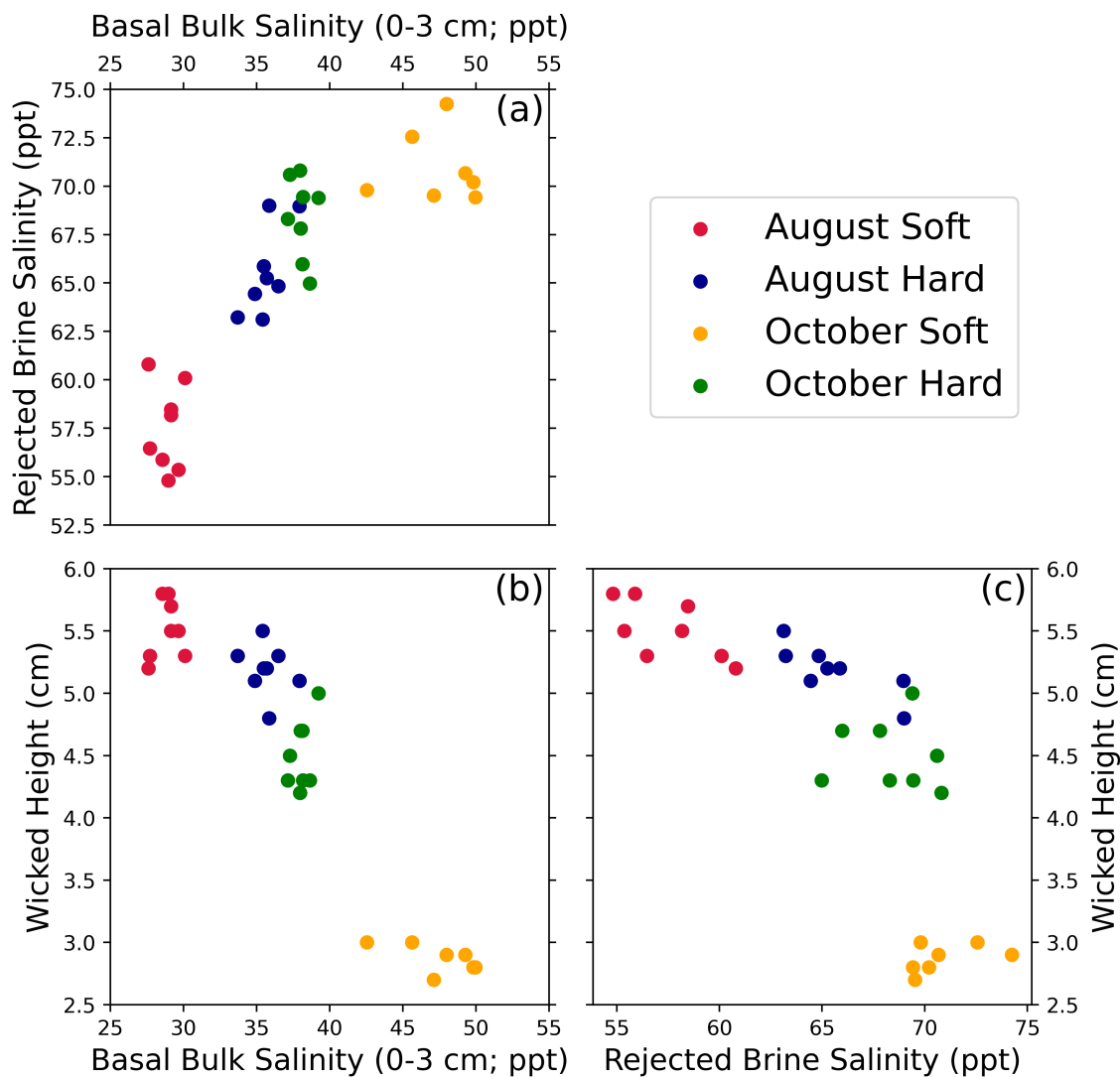


Fig. 5. Relationships between wicked height, the bulk salinity of the sample's basal 3 cm, and the brine that was released into the sample container. Clear relationships exist: a higher wicked height is associated with less salt in the base of the sample, and more diluted released brine.

302 The reduction in the basal bulk salinity over the nine day period indicates that there is less salt by
303 weight in the bottom three centimetres of the sample. So where does the salt go? One pathway is up: the
304 brine travels further up into the sample, out of the 0 - 3 cm basal layer to heights above. This explains
305 the strong correlation between wicked height and basal bulk salinity. However, another potential pathway
306 is downwards: we observed the release of dyed brine from the base of the samples several days after the
307 brine was initially added. The released brine was weighed and its salinity was measured. The mean values
308 of the four layers were 65.6, 57.5, 70.9 & 68.4 ppt, and the corresponding weights were 58.8, 20.2, 27.37 &
309 15.74 g. The salinity of the released brine was therefore much more saline but also well correlated with the
310 basal bulk salinity (Figure 5a; $r = 0.85$, slope = 1.05 ppt of salinity in the released brine for every 1 ppt
311 of salinity in the basal bulk snow). We will later discuss to what degree the salinity of the released brine
312 might reflect the salinity of the liquid phase in the bulk snow volume above.

313 We finally turn to the timescale on which the brine migrates up into the snow after it is initially
314 absorbed. We took daily of measurements of the height by which the snow surface had sank relative to
315 the top of its PVC tube, and show the results in Figure 6. Figure 6 illustrates that many of the samples
316 initially adhered to the sides of the tubes, and thus did not sink immediately. This was particularly the
317 case for the experiments in October. The data on sinking rates also show that many of the samples were
318 still sinking at the end of our nine-day experiment. This appears to particularly be the case with October's
319 soft layer, where samples settled by an average of 7 mm on the final day of the experiment. If we assume
320 that a sample's sinking rate corresponds to the wicking rate, the fact that October's soft samples were still
321 sinking when dissected may explain why the wicking heights were so much lower than for the soft snow in
322 August (Figure 4). We do not have an obvious explanation for why the October soft snow samples were
323 so much slower to wick and sink than in August, however we do point out that the density and derived
324 specific surface area of the samples was much lower (Figure 4).

325 We have avoided describing the sinking of the brine-wetted snow as *settling* here because the brine might
326 make the process quite different from the settling of dry snow (see Bernard and others, 2023, for a recent
327 summary). We investigated this difference during the second round of our experiments by monitoring
328 the 'control' settling rate of dry snow samples that were left brine-free (dashed lines in Figure 6). This
329 could then be compared to the rate at which the brine-wetted samples from the same snow layers sank.
330 Settlement of the dry snow samples is shown by dashed lines in Figure 6. At the end of the October
331 experiment the soft and hard dry snow samples had settled by 1.8 cm and 0.8 cm respectively (9.4 & 4.2%

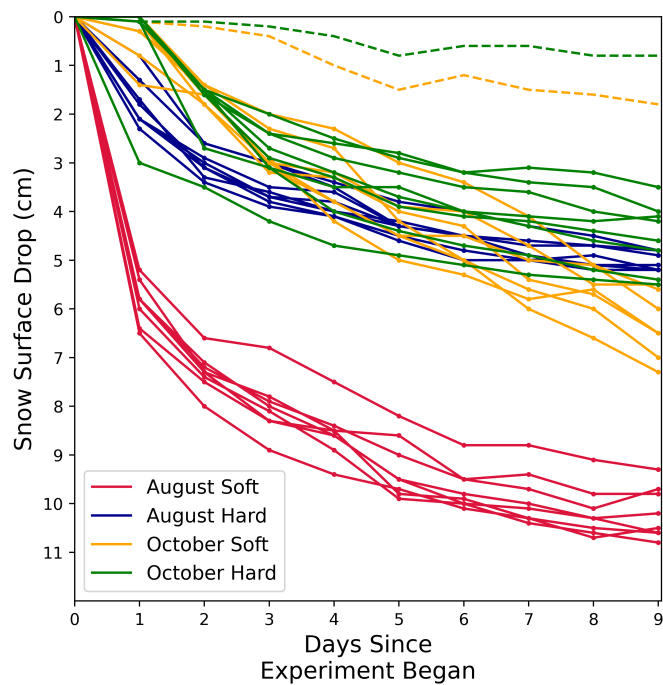


Fig. 6. The distance descended by the snow surface in all samples, measured from upper rim of the black plastic tube which was the original position of the snow surface when brine was added at the base. Solid lines indicate brine-wetted samples, dashed lines indicate control samples that were left brine-free during the second round of experiments.

332 of the initial 19 cm sample height). For comparison, the mean sinking of the soft and hard samples with
333 brine were 6.3 & 4.5 cm respectively (33 & 24%). This supports the notion that significant microstructural
334 reconfiguration is attributable to the brine, causing faster sinking than the dry-snow settling rate.

335 **Churchill Field Experiments**

336 The two sea ice sites (DP1 & DP2) had considerably different basal snow salinities. While both have
337 decreasing snow salinities with height on all days that the accumulated snow was characterised, on the
338 dates when both sites had the basal snow salinity (<4 cm) measured, the results showed salinity at DP1
339 was an order of magnitude larger than at DP2.

340 We found the basal snow salinity at both pits increased with time (Figure 8). At DP1 this is in contrast
341 to the ice surface salinities underlying the snow pits, which decreased over time (not shown). The initial
342 ice surface salinity at DP1 when the dye was deployed on 4th December was 15.12 ppt, and subsequently
343 the ice surface salinities were measured at 13.11, 10.25 & 6.5 ppt on the 9th, 11th and 12th of December.
344 These measurements were taken in a similar fashion to the snow: samples were scraped into bags, then
345 melted and analysed in the lab. As the ice underlying DP1 became fresher by 6.6 ppt, the snowpack base
346 became saltier by 3 ppt. At DP2 the ice surface salinity was initially 4.85 ppt when the dye was applied
347 on the 9th of December, and was subsequently 4.22 and 6.25 ppt on the 11th and 12th of December.

348 Because the dye at DP1 was deployed as a linear feature (Fig. 2a), we were able to observe what was
349 significant lateral migration of the dye (visible in Fig 7 a, b & c). From the photographs, it appears that
350 the dye can migrate two or three times the distance laterally than it can vertically .

351 The lake ice control experiment (CP) was deployed on the same day as DP1, but observed on 2021-
352 12-13, the day after the final measurements of the sea ice pits. As such, the dye at the control site was
353 allowed more time to migrate than either of the sea-ice based pits. Upon digging a snow pit, we observed
354 no measurable upward migration. Snow and ice salinities from CP confirmed that both the snow and ice
355 were fresh to within the measurement accuracy of the instrument and method. We also observed while
356 taking scrapings of the lake ice surface that the dye had not penetrated into the ice at all. However at the
357 sea ice, the dye had penetrated at least one centimetre.

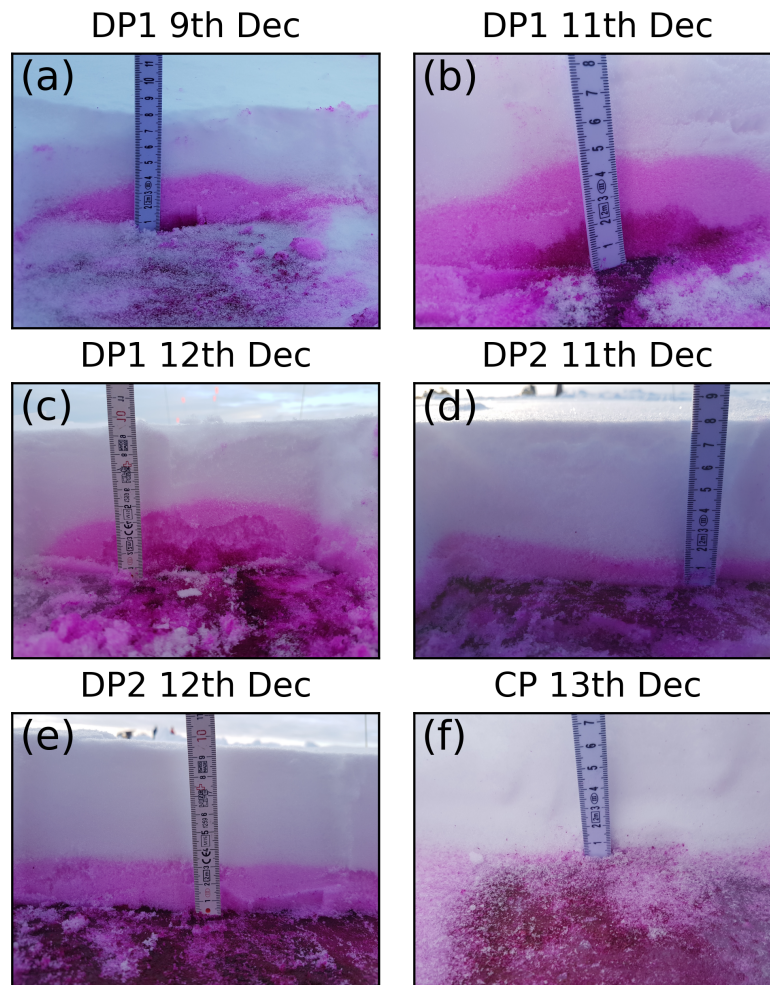


Fig. 7. Photographs showing the results of the brine wicking experiments (a - e) and the control experiment on lake ice (f). Dye was deployed at DP1 on the 4th December, and at DP2 & CP on the 9th. Upward migration of the dye into the snow is clearly visible over the sea ice, but is not in evidence on the lake ice, where the ice remained strongly dyed but the snow above was not. Significant lateral migration of the dye was visible at DP1 where the dye was originally deployed along a line.

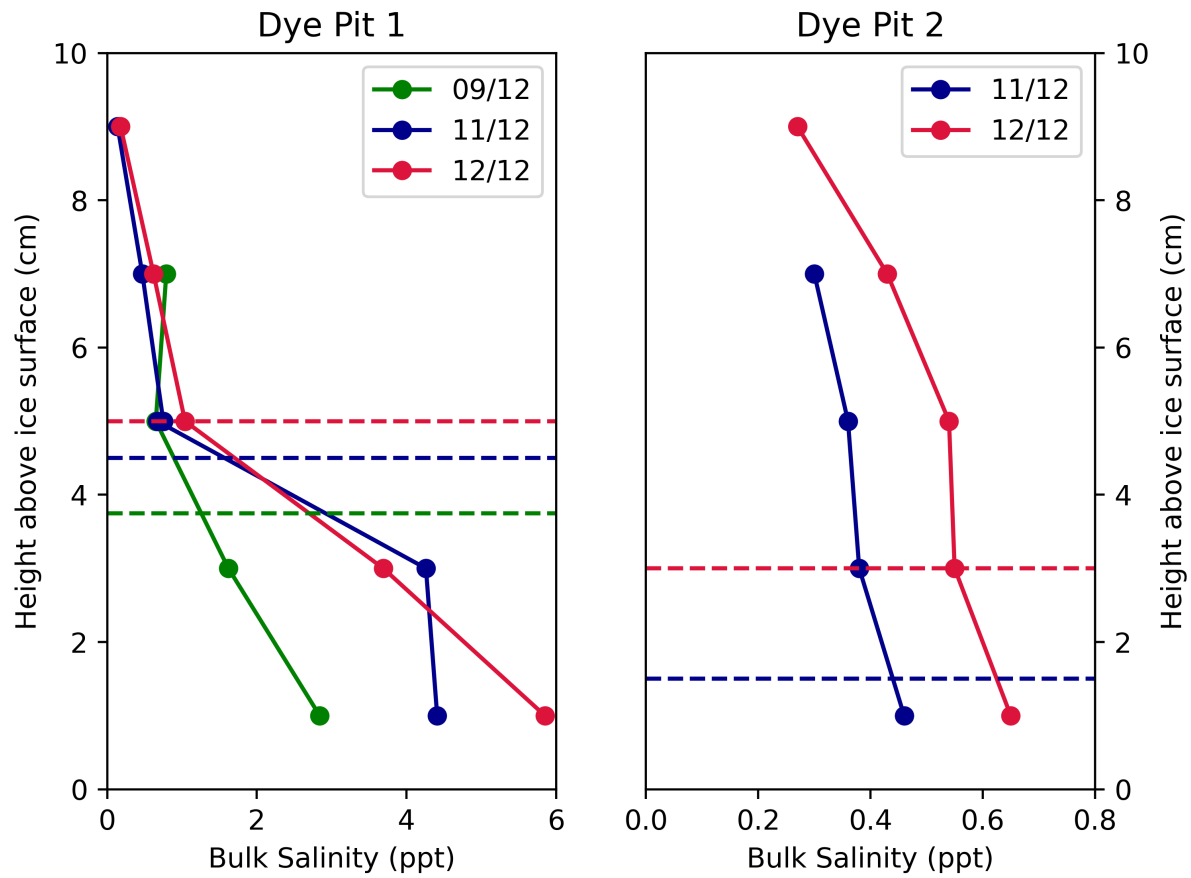


Fig. 8. Snow salinity profiles for the two sea ice sites on the dates they were visited. Horizontal dashed lines show the height to which dye had migrated by a given date. The height travelled by the dye increased day by day at both pits, as did the snow salinity values.

358 **DISCUSSION**359 **Laboratory Experiments**

360 Based on our laboratory results, we now quantify what fraction of the snow samples' pore space might
 361 have been initially filled. The volumetric fraction of air in dry snow (sometimes called the porosity, P) in
 362 a snow sample depends on its density (e.g. Essery and others, 2013):

$$P = 1 - \frac{\rho_s}{\rho_{ice}} \quad (2)$$

363 Where ρ_s is the specific gravity of the snow (i.e. the snow density as measured with our density
 364 cutter divided by the density of water), and ρ_{ice} is the density of pure ice which we take here to be 917
 365 kgm^{-3} (Fukusako, 1990). Based on Eqn. 2, the volumetric fractions of air in our four snow layers (August
 366 Soft/Hard, October Soft/Hard) are 0.74, 0.59, 0.84 & 0.83. If we then assume that the 50 millilitres of brine
 367 undergoes no dilution instantaneously, we can calculate the fraction of the snow's pore space occupied by
 368 considering the wicking heights of the samples and the dimensions of the container. We first note that the
 369 pore space available is simply P multiplied by the volume of snow that experiences wicking. This volume
 370 can be expressed as the cross-sectional area of the pipe (A) multiplied by the wicking height (W_h). The
 371 fraction of the original snow pore spaces taken up by the brine (F_{pore}) after wicking is therefore:

$$F_{pore} = \frac{B_{vol}}{W_h \times A \times P} \quad (3)$$

372 Where B_{vol} is the volume of added brine (in this case 50 ml), W_h is the observed wicking height upon
 373 immediate dissection, A is the cross-sectional area of the sample (in this case 0.031 m^2), and P is the
 374 original porosity of the dry snow sample per Eqn. 2. Taking the average of the initially checked samples
 375 in round 1, we find that the initial fraction of the pore spaces taken up (F_{pore}) are (Aug Soft/Hard, Oct
 376 Soft/Hard): 60%, 78%, 87% & 99%. This is a strikingly large range of values, and the values are not
 377 correlated with the SSA or density measurements made on the respective layers.

378 We might speculate that the fraction of the pore space initially taken up by the brine may reflect the
 379 connectivity of the pores for which air-permeability would be a proxy. In the case where pore spaces are
 380 highly connected, it is possible that the brine will occupy more of the available air space and thus not
 381 wick as high. However, the nature of the ensuing phase equilibrium between the ice and the brine within

382 the snow means that the ice is constantly melting and refreezing; this process would likely transform the
383 microstructure and thus the pore connectivity. If it is indeed the case that the brine initially wicks higher in
384 snow with a higher fraction of isolated pores that cannot be filled with brine, then we might expect that the
385 subsequent microstructural transformation would allow these pores to be filled and suppress subsequent
386 upward wicking. In fact, it does not appear that the August samples (which experienced higher initial
387 wicking) experienced less upward wicking over time.

388 We now discuss the strong correlation (but offset values) between the salinity of the released brine and
389 the salinity of the liquid phase in the bulk snow volume above (Figure 5). First we might wonder how the
390 brine compares to the equilibrium brine salinity. To do this we might assume that after nine days we have
391 reached a full phase-equilibrium between the brine and the ice; Eqn. 1 indicates that at the temperature
392 of the freezer the equilibrium brine salinity is 94 ppt, which is considerably higher than the brine that
393 was released (values between 50 and 75 ppt). Furthermore, the pink coloring of the immediately dissected
394 samples was much more vivid than in the samples dissected after nine days, indicating a significant degree
395 of dilution of brine within the sample, beyond what would be expected from a transition of our 100 ppt
396 brine to an equilibrium salinity of 94 ppt. This suggests that Equation 1 (which was derived from sea ice
397 observation) may not be fully applicable to the brine-in-snow scenario. It is important to note however
398 that the released brine was often partially frozen in the weighing boat by the time it was removed and
399 measured after nine days. In this sense, we are measuring the salinity of what may be viewed as a bulk
400 sample, and not the salinity of a purely liquid brine in an equilibrium with unmeasured ice per Eqn 1.

401 **Churchill Field Experiments**

402 The evolution of the salinity profiles over sea ice are of interest independently of the dye behaviour.
403 It appears that even in cold conditions ($<-10^{\circ}\text{C}$; Figure 2c), accumulating snow on sea ice generates a
404 characteristic monotonic profile, and that this profile can evolve in a matter of days. This is novel, as
405 most studies have looked at increases in snow salinity over new ice in comparatively warm conditions (see
406 Dominé and others, 2004, for discussion of this).

407 A potential challenge to the above analysis involves the lateral variability in ice surface salinity. One can
408 imagine that as we dug snow pits along the ice over time, we inadvertently sampled increasingly saline ice
409 due to lateral variability which induced increasingly saline snow even in the absence of any time-evolution
410 of the system. We argue that the *decreasing* ice surface salinity of the DP1 pits over time indicates that

411 this is not the case (with DP2 being relatively inconclusive in this regard).

412 Turning to the observed dye heights, they increased over time along with the snow salinity values.
 413 Although we do not have enough data to investigate whether larger increases in the basal salinity were
 414 associated with larger increases in the wicked height, the fact that we saw no dye migration at the lake
 415 site where there was no snow salinity is encouraging. This suggests that the development of both pits'
 416 characteristic monotonic salt profile is at least in part directly driven by upward migration of brine from
 417 the ice surface. While some of the salt may be deposited from the atmosphere, or be delivered with the
 418 snow that was blown into the trench, there is only one source of dye: the ice surface. For dye to move up
 419 into the snow, we conclude it must have migrated upwards from there via a liquid water pathway.

420 The fact that the dye was able to travel upwards at all in such cold temperatures and low bulk salinities
 421 is perhaps surprising, particularly for DP2. Using the bulk salinity of the snow and coincident temperature
 422 measurements of the layers, we can estimate the brine volume fraction (BVF) of the snow using Equation
 423 3 from Frankenstein and Garner (1967):

$$BVF = S_{bulk} \left(\frac{45.917}{-T_s} + 0.93 \right) \quad (4)$$

424 Where S_{bulk} and T_s are the bulk salinity and temperature of the snow layer in question. In order to
 425 calculate an upper-bound on the snow BVF, we consider the basal (bottom 2 cm) snow layers of DP1 &
 426 DP2, which were consistently the warmest and most saline. At DP1 we calculate increasing BVF values
 427 of 1.7, 2.8 and 4.5% on the 9th, 11th and 12th of December respectively (Table 1). At DP2 these values
 428 are an order of magnitude lower (due to the much lower bulk salinities), at 0.3 & 0.5% for the 11th and
 429 12th of December respectively. Given the BVFs are so much lower, it is noteworthy that the dye wicking
 430 height is not suppressed by a similar factor.

431 Work by Denoth (1980) indicates that the transition of fresh liquid water from the pendular to the
 432 funicular regime in the range of 11-15% of the pore volume (not the BVF). We can convert BVF values to
 433 the fraction of the pore volume filled by calculating the porosity of the basal snow following a version of
 434 Eqn 2 modified for the presence of the brine itself, following Section 2.2 of Geldsetzer and others (2009):

$$P = 1 - \frac{\rho_s - (BVF \times \rho_b)}{\rho_{ice}} \quad (5)$$

435 Where all variables have the same definitions as in Eqn. 2 and ρ_b represents the density of the brine,

Table 1. Values used in the calculation of the fraction of the available pore space taken up by brine at DP1 & DP2. BVF refers to brine volume fraction per Eqn. 4. P refers to porosity per Eqn. 5. Values for BVF/P generally do not exceed the threshold for the transition to the funicular regime given by Denoth (1980).

| Pit | Date | Temperature (°C) | BVF (%) | Density (kg/m ³) | P | BVF/P (%) |
|-----|----------------------|------------------|---------|------------------------------|------|-----------|
| DP1 | 9 th Dec | -8.92 | 1.73 | 154 | 0.83 | 2.07 |
| DP1 | 11 th Dec | -8.40 | 2.82 | 255 | 0.72 | 3.91 |
| DP1 | 12 th Dec | -6.86 | 4.46 | 223 | 0.76 | 5.89 |
| DP2 | 11 th Dec | -7.80 | 0.31 | 185 | 0.80 | 0.39 |
| DP2 | 12 th Dec | -6.34 | 0.53 | 194 | 0.79 | 0.67 |

436 which we calculate using Eqn 16 of Cox and Weeks (1975):

$$\rho_b = 1 + 0.0008S_b \quad (6)$$

437 To calculate the fraction of the pore space taken up by the brine, we divide the brine volume fraction
 438 (Eqn 4) by the brine-adjusted porosity (Eqn. 5). Because of the low BVF values we find that adjusting the
 439 porosity calculation shown in Eqn. 2 for the brine weight does not make a difference to the three significant
 440 figures of precision shown in Table 1. In the basal snow layers the fraction of the pore space filled by brine
 441 (BVF/P column of Table 1) is generally around 20 - 40% larger than the brine volume fraction values
 442 themselves; the largest values for both pits occur on the 12th of December and are 5.8 & 0.67% for DP1
 443 & DP2 respectively (see Table 1). These values are well short of the 11% described by Denoth (1980) for
 444 shifting from the pendular to funicular regime. However, we note that those values are for *fresh* water in
 445 snow, which may have a different microscopic arrangement due to transformation of the microstructure by
 446 the brine. Our results indicate that vertical liquid pathways of several centimetres length do exist from
 447 the snow/ice interface into the snow volume, even at low salinity values and temperatures.

448 One uncertainty in this technique concerns whether the dye always traces the upward flux of brine,
 449 or simply illuminates pathways of interconnected brine pockets by diffusion. In the fieldwork presented
 450 here we were able to measure consistently increasing snow salinity so it does appear that the sign of the
 451 brine flux was at least positive in the upward direction, even if the magnitude was small at DP2. We
 452 do therefore raise the possibility that the presence of salt produced a series of thin, interconnected liquid
 453 films through which the dye was able to diffuse in the absence of significant bulk movement of liquid. The

454 control experiment indicates that this is only possible in the presence of salt, and that the snow's inherent
455 quasi-liquid layers are not sufficient for the brine to diffuse if this indeed occurs at all. In the photographs
456 of DP1 presented in Figure 7 there is a visible two-tone pattern of a darker shade of dye below a lighter
457 shade. We were unable to identify a root cause of this pattern, which is not visible at DP2 where the colour
458 was relatively uniform over the dyed area of snow. However we do note that the ice at DP1 was smoother
459 than the ice at DP2, and the dye was much more abundantly deployed at DP1 because the spray-gun was
460 not used.

461 Results from DP1 indicate that the dye migrated further horizontally than it did vertically. One simple
462 explanation for this is that the dye moved horizontally through the top layer of the ice (which has a
463 substantial liquid water component even in cold conditions), and then moved vertically up through the
464 snow. However if this is not the case and the dye did indeed move substantially through the snow in
465 a lateral direction, it raises questions about the role of snow's microstructural anisotropy in brine/dye
466 wicking. This is of interest when considering the fact that we rotated the snow samples in our laboratory
467 experiments, and dye was wicking against gravity but laterally through the snow with respect to its initial
468 orientation.

469 **Experimental Constraints and Future Directions**

470 Our snow samples in the laboratory were produced by horizontally driving pipes into distinct stratigraphic
471 layers that we observed. We then rotated the pipes so that brine could be introduced at the base, meaning
472 the snow was no longer in the orientation in which it accumulated. If the snow had significant microstruc-
473 tural anisotropy, then this will have diminished the realism of our experiments. Furthermore, if the snow
474 has small-scale vertical layering in-situ then that may contribute to horizontal variability in the wicked
475 height once the sample has been rotated. Our results showed that wicking did not exceed 7 cm in height, so
476 our 19 cm sampling tubes were excessively long for this experiment. In future the tubes could potentially
477 be inserted vertically if a homogenous stratigraphic snow layer of sufficient thickness to accommodate the
478 wicking is found. It would also be valuable to study how snow stratigraphy controls brine wicking, as a
479 layered structure is commonly observed in a natural snow-covered sea ice environment.

480 Our freezer did not have a reliably adjustable thermostat, so we carried out all our work at a fixed tem-
481 perature of around -5.6°C . Furthermore, there was some temperature cycling due to the gas-thermostat's
482 control over the compressor. While the real environment of course fluctuating air temperature on various

483 timescales, removing the temperature cycling inside the freezer would be desirable as it would simplify the
484 physics. Furthermore, it would be very instructive to perform the same suite of experiments at different
485 temperatures, as this would control the equilibrium salinity and brine volume fraction inside the snow.

486 We performed our experiment at $\sim -5.6^{\circ}\text{C}$, and therefore used a high salinity (100 ppt) brine. While
487 this brine may reflect realistic values for a brine skim formed through upward brine rejection, it is unrepresentative
488 of the salinity of the seawater that can flood the base of the snowpack. Incidentally, the amount
489 of brine supplied exceeds that which would be supplied by a brine skim. Future research on brine-wicking
490 after flooding should therefore aim to use a more appropriate brine salinity such as that of real ocean water.
491 This would require careful operation at a higher temperature ($> -1.8^{\circ}\text{C}$) to allow the brine to be added at
492 the same temperature as the snow.

493 We were only able to characterise the snow microstructure using the snow micropenetrometer, and we
494 have assumed that its sampling of the snow layers from which the samples were taken accurately reflects the
495 snow samples themselves. This may not be the case, especially if the snow samples undergo microstructural
496 metamorphosis inside the freezer. To investigate the potential for this, we first attempted to drive the SMP
497 through the snow samples in their tubes; we found that due to the conical shape of the probe, snow was
498 forced against the sides of the tube and readings were unreliable. We also measured the degree of settling
499 of two dummy samples (one from hard snow, and one from soft snow) which did not have brine added to
500 them during the second round of experiments. We found that over the nine days, the soft snow sank 1.8 cm
501 into the tube, and the hard snow sank 0.8 mm. Assuming the mass of snow was conserved, this corresponds
502 to an increase in the density of the snow samples of 9.4 and 4.2% respectively. This densification is likely
503 caused by microstructural change, and this would ideally be monitored with a method such as micro-CT
504 scanning in future. However, we did not quantify the role of snow sublimation over the experiment. As
505 well as affecting the densification, sublimation may also have changed the microstructure from that which
506 was measured by the SMP. Sublimation could be monitored in future by weighing the samples at regular
507 intervals during the experiment, and noting any reductions in mass.

508 As for the brine-filled samples, micro-CT scanning may be able to resolve the exact microstructural
509 configuration of the snow after being in contact with the brine. It also has the potential to image exactly
510 how much of the pore volume remains available both after initial wicking and after nine days. Furthermore,
511 it could resolve the previously posed questions regarding the original connectivity of the pore structures
512 in the snow. Finally, and most critically, micro-CT scanning is a non-destructive technique which sharply

513 contrasts with our dissection-based approach. It would make it possible to monitor the migration of brine
514 up a sample over time without destroying it.

515 **Field Constraints and Future Directions**

516 Sea ice can generally only be travelled when the ice is thick enough to support humans. By the time this
517 is the case and the weather conditions are suitable, it has often already accumulated snow and/or frost
518 flowers. In order to place dye on the ice surface before snow falls on it, the use of a small boat is likely
519 necessary. An alternative would be the use of an artificial sea ice mesocosm (sometimes referred to as a
520 *sea ice tank*). These facilities often feature gantries from which dye could be applied in the early stages of
521 sea ice formation.

522 The means by which the dye was applied to the sea ice surface could be improved relative to the
523 setup reported here. For both the lab and the field experiments, the quantity of the dye deployed was not
524 controlled, so perceived dilution later could only be qualitatively identified. Furthermore, the application
525 with the spray-gun was patchy rather than even. In future, low volume spray nozzles could be used to
526 apply dye evenly.

527 **SUMMARY**

528 We have presented results from lab and field experiments using rhodamine-WT dye to trace the upward
529 movement of brine in snow. Our lab experiments differed from the field because we actively supplied brine
530 alongside the dye, leading to a larger initial volume of liquid in the snow, with commensurately higher bulk
531 salinities. Despite their differences, both settings exhibited obvious upward migration of the dyed brine,
532 indicating that the phenomenon occurs in comparatively dry and wet snow regimes.

533 Our results are not trivial to interpret. This is particularly the case in the lab, where snow density
534 and specific surface area estimates did not appear to be related to the height to which the dye wicked,
535 either initially or on a multi-day timescale. Despite brine being added to the snow base at close to its
536 equilibrium salinity, a more diluted brine was released from the base of the samples after several days. We
537 attribute the rejection to salinity-driven microstructural metamorphosis which made the snow less capable
538 of holding liquid.

539 Our control experiment from the field indicated that saline ice was required for the dye to migrate
540 upwards. The dye migrated several centimetres up into the snow even when snow salinity measurements

Mallett and others:

541 implied that <1% of the pore space was occupied by brine; the exact way in which this occurred remains
542 unknown, but could be resolved in future with micro-CT imaging.

543 **ACKNOWLEDGEMENTS**

544 This work was funded in part by the Canada 150 Research Chairs Programme (Grant 50296), providing
545 funding for RM, VN, JS, RW and MS. RM was additionally supported by the NERC Doctoral Training
546 Partnership (NE/L002485/1) during the field experiments in Churchill, while RM, JS, RW, GV and JW
547 also received funding from the NERC DEFIANT grant (NE/W004739/1) in support of data collection and
548 analysis at Rothera Station. RW and JS also received funding from the European Union's Horizon 2020
549 research and innovation programme via project CRiceS (Grant 101003826).

550 **CODE AND DATA AVAILABILITY**

551 **AUTHOR CONTRIBUTIONS**

552 RM and VN conceived the protocols, led the field study, and performed the lab work at Rothera research
553 station. RW, JS, JY and MS contributed to the Churchill field campaign, including gathering the snow pit
554 data and analysing snow samples. JW & GV contributed feedback and conceptualisation of the lab study.
555 All authors contributed to the final manuscript.

556 **REFERENCES**

- 557 Babb DG, Galley RJ, Kirillov S, Landy JC, Howell SEL, Stroeve JC, Meier W, Ehn JK and Barber DG (2023) The
558 Stepwise Reduction of Multiyear Sea Ice Area in the Arctic Ocean Since 1980. *Journal of Geophysical Research:*
559 *Oceans*, **128**(10), e2023JC020157, ISSN 2169-9291 (doi: 10.1029/2023JC020157)
- 560 Barber DG and Nghiem SV (1999) The role of snow on the thermal dependence of microwave backscatter over sea ice.
561 *Journal of Geophysical Research: Oceans*, **104**(C11), 25789–25803, ISSN 2156-2202 (doi: 10.1029/1999JC900181)
- 562 Barber DG, Fung AK, Grenfell T, Nghiem S, Onstott R, Lytle V, Perovich D and Gow A (1998) The role of snow on
563 microwave emission and scattering over first-year sea ice. *IEEE Transactions on Geoscience and Remote Sensing*,
564 **36**(5 PART 2), 1750–1763, ISSN 01962892 (doi: 10.1109/36.718643)
- 565 Barber DG, Iacozza J and Walker AE (2003) Estimation of snow water equivalent using microwave radiometry over
566 Arctic first-year sea ice. *Hydrological Processes*, **17**(17), 3503–3517, ISSN 08856087 (doi: 10.1002/hyp.1305)

- 567 Bennington KO (1967) Desalination Features in Natural Sea Ice. *Journal of Glaciology*, **6**(48), 845–857, ISSN 0022-
568 1430 (doi: 10.3189/s0022143000020153)
- 569 Bernard A, Hagenmuller P, Montagnat M and Chambon G (2023) Disentangling creep and isothermal metamorphism
570 during snow settlement with X-ray tomography. *Journal of Glaciology*, **69**(276), 899–910, ISSN 0022-1430 (doi:
571 10.1017/JOG.2022.109)
- 572 Butler BM, Papadimitriou S, Santoro A and Kennedy H (2016) Mirabilite solubility in equilibrium sea ice brines.
573 *Geochimica et Cosmochimica Acta*, **182**, 40–54, ISSN 0016-7037 (doi: 10.1016/J.GCA.2016.03.008)
- 574 Confer KL, Jaeglé L, Liston GE, Sharma S, Nandan V, Yackel J, Ewert M and Horowitz HM (2023) Impact of
575 Changing Arctic Sea Ice Extent, Sea Ice Age, and Snow Depth on Sea Salt Aerosol From Blowing Snow and
576 the Open Ocean for 1980–2017. *Journal of Geophysical Research: Atmospheres*, **128**(3), e2022JD037667, ISSN
577 2169-8996 (doi: 10.1029/2022JD037667)
- 578 Cox GF and Weeks WF (1975) Brine drainage and initial salt entrapment in sodium chloride ice. *US Army Corps*
579 *Eng Cold Reg Res Eng Lab Res Rep*, (345)
- 580 Crocker GB (1984) A physical model for predicting the thermal conductivity of brine-wetted snow. *Cold Regions*
581 *Science and Technology*, **10**(1), 69–74, ISSN 0165-232X (doi: 10.1016/0165-232X(84)90034-X)
- 582 Davis RE and Dozier J (1984) Snow Wetness Measurement by Fluorescent Dye Dilution. *Journal of Glaciology*,
583 **30**(106), 362–363, ISSN 0022-1430 (doi: 10.3189/S0022143000006225)
- 584 Denoth A (1980) The Pendular-Funicular Liquid Transition in Snow. *Journal of Glaciology*, **25**(91), 93–98, ISSN
585 0022-1430 (doi: 10.3189/S0022143000010315)
- 586 Dominé F and Shepson PB (2002) Air-snow interactions and atmospheric chemistry. *Science*, **297**(5586), 1506–
587 1510, ISSN 00368075 (doi: 10.1126/SCIENCE.1074610/ASSET/D6C41CA3-8555-4C68-BB61-9BAE445F0944/
588 ASSETS/GRAPHIC/SE3420818004.JPEG)
- 589 Dominé F, Sparapani R, Ianniello A and Beine HJ (2004) The origin of sea salt in snow on Arctic sea ice and in
590 coastal regions. *Atmospheric Chemistry and Physics Discussions*, **4**(4), 4737–4776, ISSN 16807316 (doi: 10.5194/
591 acpd-4-4737-2004)
- 592 Drinkwater MR and Crocker GB (1988) Modelling changes in the dielectric and scattering properties of young
593 snow-covered sea ice at GHz frequencies. *Journal of Glaciology*, **34**(118), 274–282, ISSN 00221430 (doi: 10.3189/
594 s0022143000007012)
- 595 Eide LI and Martin S (1975) The Formation of Brine Drainage Features in Young Sea Ice. *Journal of Glaciology*,
596 **14**(70), 137–154, ISSN 0022-1430 (doi: 10.3189/S0022143000013460)

Mallett and others:

- 597 Essery R, Morin S, Lejeune Y and B Ménard C (2013) A comparison of 1701 snow models using observations from
598 an alpine site. *Advances in Water Resources*, **55**, 131–148, ISSN 03091708 (doi: 10.1016/j.advwatres.2012.07.013)
- 599 Frankenstein G and Garner R (1967) Equations for Determining the Brine Volume of Sea Ice from -0.5C to -22.9C.
600 *Journal of Glaciology*, **6**(48), 943–944, ISSN 0022-1430 (doi: 10.3189/S0022143000020244)
- 601 Freitag J and Eicken H (2003) Meltwater circulation and permeability of Arctic summer sea ice derived from hydrologi-
602 cal field experiments. *Journal of Glaciology*, **49**(166), 349–358, ISSN 0022-1430 (doi: 10.3189/172756503781830601)
- 603 Frey MM, Norris SJ, Brooks IM, Anderson PS, Nishimura K, Yang X, Jones AE, Nerentorp Mastromonaco MG,
604 Jones DH and Wolff EW (2020) First direct observation of sea salt aerosol production from blowing snow above
605 sea ice. *Atmospheric Chemistry and Physics*, **20**(4), 2549–2578, ISSN 16807324 (doi: 10.5194/ACP-20-2549-2020)
- 606 Fukusako S (1990) Thermophysical properties of ice, snow, and sea ice. *International Journal of Thermophysics*,
607 **11**(2), 353–372, ISSN 0195928X (doi: 10.1007/BF01133567)
- 608 Geldsetzer T, Langlois A and Yackel J (2009) Dielectric properties of brine-wetted snow on first-year sea ice. *Cold*
609 *Regions Science and Technology*, **58**(1-2), 47–56, ISSN 0165232X (doi: 10.1016/j.coldregions.2009.03.009)
- 610 Gong X, Zhang J, Croft B, Yang X, Frey MM, Bergner N, Chang RY, Creamean JM, Kuang C, Martin RV, Ran-
611 jithkumar A, Sedlacek AJ, Uin J, Willmes S, Zawadowicz MA, Pierce JR, Shupe MD, Schmale J and Wang J
612 (2023) Arctic warming by abundant fine sea salt aerosols from blowing snow. *Nature Geoscience* 2023 16:9, **16**(9),
613 768–774, ISSN 1752-0908 (doi: 10.1038/s41561-023-01254-8)
- 614 Industrial Process Measurement Inc (2016) Water Quality Meters; Oakton Waterproof pH 450, CON 450 and
615 pH/CON 450 Meters. Technical report, [https://www.instrumentation2000.com//media/pdf/oakton-ph-con-450-](https://www.instrumentation2000.com//media/pdf/oakton-ph-con-450-datasheet.pdf)
616 [datasheet.pdf](https://www.instrumentation2000.com//media/pdf/oakton-ph-con-450-datasheet.pdf)
- 617 Liston GE, Itkin P, Stroeve J, Tschudi M, Stewart JS, Pedersen SH, Reinking AK and Elder K (2020) A Lagrangian
618 Snow-Evolution System for Sea-Ice Applications (SnowModel-LG): Part I – Model Description. *Journal of Geo-*
619 *physical Research: Oceans*, **125**(10), e2019JC015913, ISSN 2169-9275 (doi: 10.1029/2019jc015913)
- 620 Markus T, Stroeve JC and Miller J (2009) Recent changes in Arctic sea ice melt onset, freezeup, and melt season
621 length. *Journal of Geophysical Research: Oceans*, **114**, C12024 (doi: 10.1029/2009JC005436)
- 622 Massom RA, Eicken H, Haas C, Jeffries MO, Drinkwater MR, Sturm M, Worby AP, Wu X, Lytle VI, Ushio S, Morris
623 K, Reid PA, Warren SG and Allison I (2001) Snow on Antarctic sea ice. *Reviews of Geophysics*, **39**(3), 413–445,
624 ISSN 1944-9208 (doi: 10.1029/2000RG000085)

- 625 Nandan V, Geldsetzer T, Islam T, Yackel JJ, Gill JP, Fuller MC, Gunn G and Duguay C (2016) Ku-, X- and C-band
626 measured and modeled microwave backscatter from a highly saline snow cover on first-year sea ice. *Remote Sensing*
627 *of Environment*, **187**, 62–75, ISSN 0034-4257 (doi: 10.1016/J.RSE.2016.10.004)
- 628 Nandan V, Geldsetzer T, Yackel J, Mahmud M, Scharien R, Howell S, King J, Ricker R and Else B (2017) Effect
629 of Snow Salinity on CryoSat-2 Arctic First-Year Sea Ice Freeboard Measurements. *Geophysical Research Letters*,
630 **44**(20), 419–426, ISSN 19448007 (doi: 10.1002/2017GL074506)
- 631 Nandan V, Scharien RK, Geldsetzer T, Kwok R, Yackel JJ, Mahmud MS, Rosel A, Tonboe R, Granskog M, Willatt
632 R, Stroeve J, Nomura D and Frey M (2020) Snow Property Controls on Modeled Ku-Band Altimeter Estimates
633 of First-Year Sea Ice Thickness: Case Studies from the Canadian and Norwegian Arctic. *IEEE Journal of Selected*
634 *Topics in Applied Earth Observations and Remote Sensing*, **13**, 1082–1096, ISSN 21511535 (doi: 10.1109/JSTARS.
635 2020.2966432)
- 636 Nicolaus M, Haas C and Willmes S (2009) Evolution of first-year and second-year snow properties on sea ice in the
637 Weddell Sea during spring-summer transition. *Journal of Geophysical Research Atmospheres*, **114**(17), D17109,
638 ISSN 01480227 (doi: 10.1029/2008JD011227)
- 639 Perovich DK and Richter-Menge JA (1994) Surface characteristics of lead ice. *Journal of Geophysical Research:*
640 *Oceans*, **99**(C8), 16341–16350, ISSN 2156-2202 (doi: 10.1029/94JC01194)
- 641 Petty AA, Webster M, Boisvert L and Markus T (2018) The NASA Eulerian Snow on Sea Ice Model (NESOSIM)
642 v1.0: Initial model development and analysis. *Geoscientific Model Development*, **11**(11), 4577–4602, ISSN 19919603
643 (doi: 10.5194/gmd-11-4577-2018)
- 644 Proksch M, Löwe H and Schneebeli M (2015a) Density, specific surface area, and correlation length of snow measured
645 by high-resolution penetrometry. *Journal of Geophysical Research: Earth Surface*, **120**(2), 346–362, ISSN 21699011
646 (doi: 10.1002/2014JF003266)
- 647 Proksch M, Mätzler C, Wiesmann A, Lemmetyinen J, Schwank M, Löwe H and Schneebeli M (2015b) MEMLS3&a:
648 Microwave Emission Model of Layered Snowpacks adapted to include backscattering. *Geoscientific Model Devel-*
649 *opment*, **8**(8), 2611–2626, ISSN 19919603 (doi: 10.5194/gmd-8-2611-2015)
- 650 Proksch M, Rutter N, Fierz C and Schneebeli M (2016) Intercomparison of snow density measurements: Bias,
651 precision, and vertical resolution. *Cryosphere*, **10**(1), 371–384, ISSN 19940424 (doi: 10.5194/TC-10-371-2016)
- 652 Provost C, Sennéchaël N, Miguet J, Itkin P, Rösel A, Koenig Z, Villacieros-Robineau N and Granskog MA (2017)
653 Observations of flooding and snow-ice formation in a thinner Arctic sea-ice regime during the N-ICE2015 campaign:
654 Influence of basal ice melt and storms. *Journal of Geophysical Research: Oceans*, **122**(9), 7115–7134, ISSN 2169-
655 9291 (doi: 10.1002/2016JC012011)

Mallett and others:

- 656 Sazaki G, Zepeda S, Nakatsubo S, Yokomine M and Furukawa Y (2012) Quasi-liquid layers on ice crystal surfaces are
657 made up of two different phases. *Proceedings of the National Academy of Sciences of the United States of America*,
658 **109**(4), 1052–1055, ISSN 00278424 (doi: 10.1073/PNAS.1116685109/SUPPL{_}_FILE/SM04.AVI)
- 659 Schneebeli M and Johnson JB (1998) A constant-speed penetrometer for high-resolution snow stratigraphy. *Annals*
660 *of Glaciology*, **26**, 107–111, ISSN 0260-3055 (doi: 10.3189/1998AOG26-1-107-111)
- 661 Smart PL and Laidlaw IM (1977) An evaluation of some fluorescent dyes for water tracing. *Water Resources Research*,
662 **13**(1), 15–33 (doi: 10.1029/WR013I001P00015)
- 663 Stogryn A (1986) A Study of the Microwave Brightness Temperature of Snow from the Point of View of Strong
664 Fluctuation Theory. *IEEE Transactions on Geoscience and Remote Sensing*, **GE-24**(2), 220–231, ISSN 15580644
665 (doi: 10.1109/TGRS.1986.289641)
- 666 Stroeve J and Notz D (2018) Changing state of Arctic sea ice across all seasons. *Environmental Research Letters*,
667 **13**(10), 103001, ISSN 17489326 (doi: 10.1088/1748-9326/aade56)
- 668 Weeks W (1968) Understanding the variations of the physical properties of sea ice. In *SCAR/SCOR/ IAPOjiUPS*
669 *Symposium on Antarctic Oceanography (Santiago, Chile, 1966)*, 173–190, SCAR/SCOR/ IAPOjiUPS Symposium
670 on Antarctic Oceanography (Santiago, Chile, 1966), Cambridge; England: Scott Polar Research Institute
- 671 Wever N, Rossmann L, Maaß N, Leonard KC, Kaleschke L, Nicolaus M and Lehning M (2020) Version 1 of a sea ice
672 module for the physics-based, detailed, multi-layer SNOWPACK model. *Geoscientific Model Development*, **13**(1),
673 99–119, ISSN 19919603 (doi: 10.5194/gmd-13-99-2020)
- 674 Willatt RC, Giles KA, Laxon SW, Stone-Drake L and Worby AP (2010) Field investigations of Ku-band radar
675 penetration into snow cover on antarctic sea ice. *IEEE Transactions on Geoscience and Remote Sensing*, **48**(1),
676 365–372, ISSN 01962892 (doi: 10.1109/TGRS.2009.2028237)
- 677 Wren SN, Donaldson DJ and Abbatt JP (2013) Photochemical chlorine and bromine activation from artificial saline
678 snow. *Atmospheric Chemistry and Physics*, **13**(19), 9789–9800, ISSN 16807316 (doi: 10.5194/ACP-13-9789-2013)
- 679 Yackel J, Geldsetzer T, Mahmud M, Nandan V, Howell SE, Scharien RK and Lam HM (2019) Snow thickness
680 estimation on first-year sea ice from late winter spaceborne scatterometer backscatter variance. *Remote Sensing*,
681 **11**(4), ISSN 20724292 (doi: 10.3390/rs11040417)

Dye tracing of upward brine migration in snow

Robbie MALLETT,^{1,2,†} Vishnu NANDAN,^{3,4,5,†} Julienne STROEVE,^{2,3,6} Rosemary WILLATT,^{7,2}
Monojit SAHA,³ John YACKEL,⁴ Gaëlle VEYSIÈRE^{2,8} Jeremy WILKINSON⁸

[†] *These authors contributed equally to this work*

¹*Earth Observation Group, Department of Physics and Technology,
UiT The Arctic University of Norway, Norway*

²*Centre for Polar Observation and Modelling, Department of Earth Sciences,
University College London, UK*

³*Centre for Earth Observation Science, University of Manitoba, Winnipeg, Canada*

⁴*Cryosphere Climate Research, Group, Department of Geography,
University of Calgary, Canada*

⁵*H2O Geomatics Inc, Kitchener, Ontario, Canada*

⁶*National Snow and Ice Data Center,*

University of Colorado, Boulder, CO, USA

⁷*Centre for Polar Observation and Modelling, Department of Geography
and Environmental Sciences, University of Northumbria, UK*

⁸*British Antarctic Survey, Cambridge, UK*

Correspondence: Robbie Mallett <robbiemallett@gmail.com>

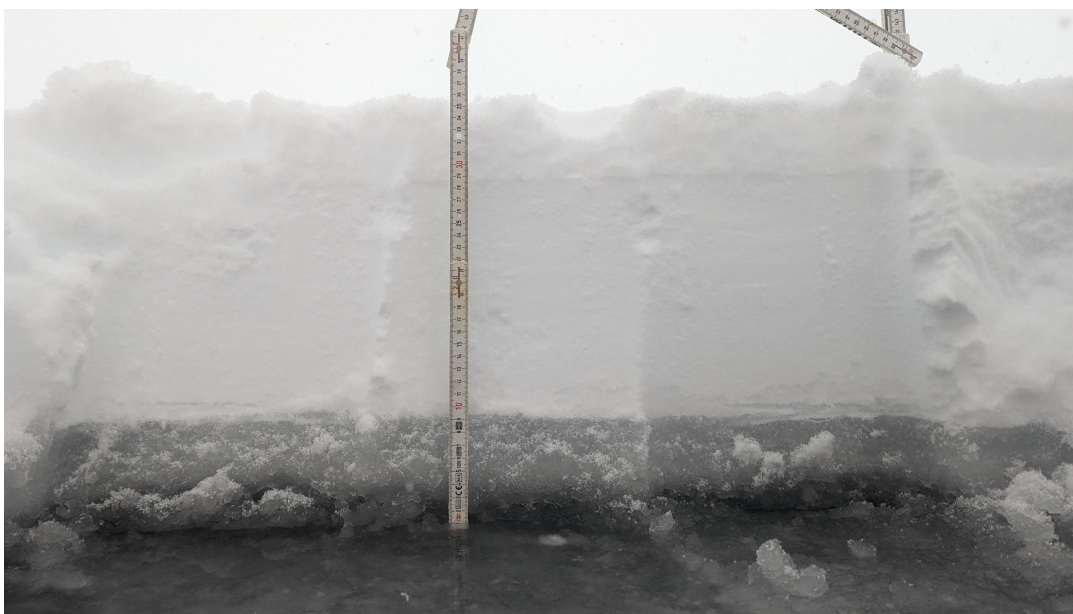


Fig. S1. Photograph of upward wicking of brine in snow over flooded sea ice taken by the authors in 2023. Snow was observed to be wet up to 9 cm above the ice, and 8 cm above the waterline. C.f. Figure 1c of the main manuscript.

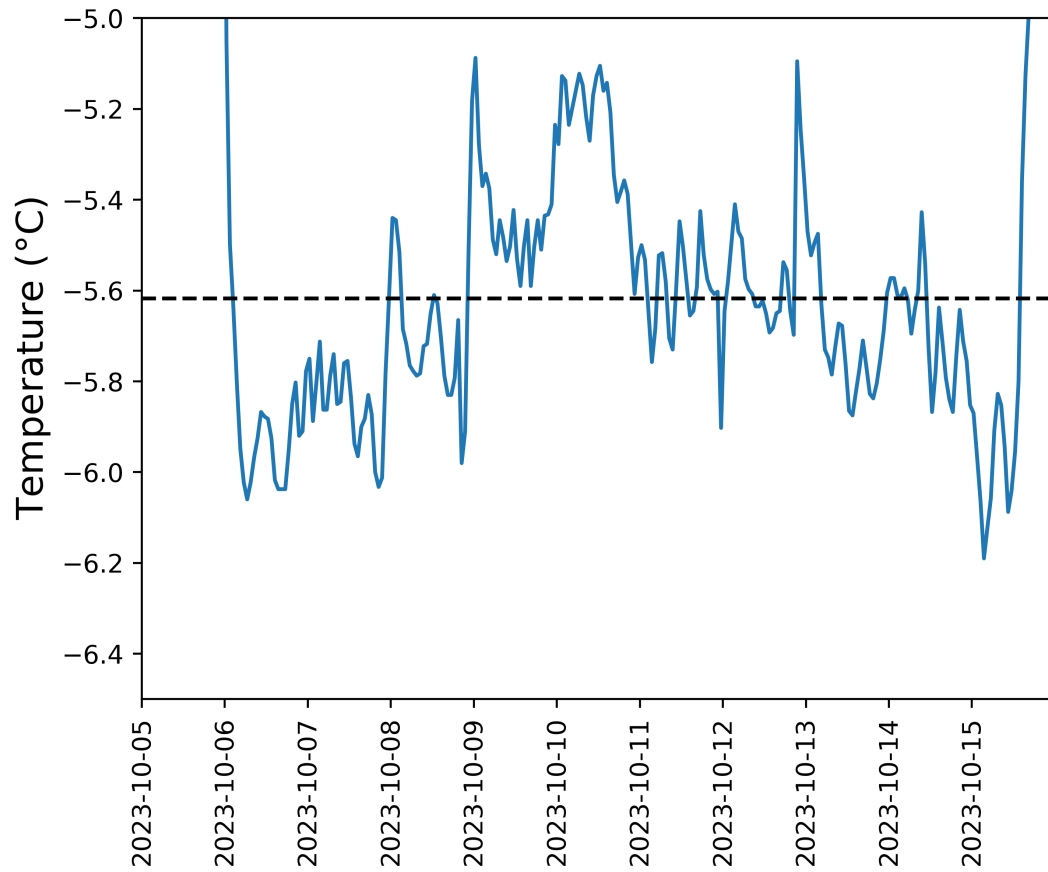


Fig. S2. Temperature fluctuations measured by a probe sandwiched inside a dummy snow sample within a PVC tube inside the freezer. Measurements began after one day in the second experimental round, in a tube that had had its sample dissected. Mean temperature measured by the probe while inside the freezer indicated by black dashed line.



Fig. S3. Photograph showing the previous setup of the experiment, where snow samples and their tubes ‘shared’ a brine supply. This led to preferential uptake from some samples and led to unreliable results.

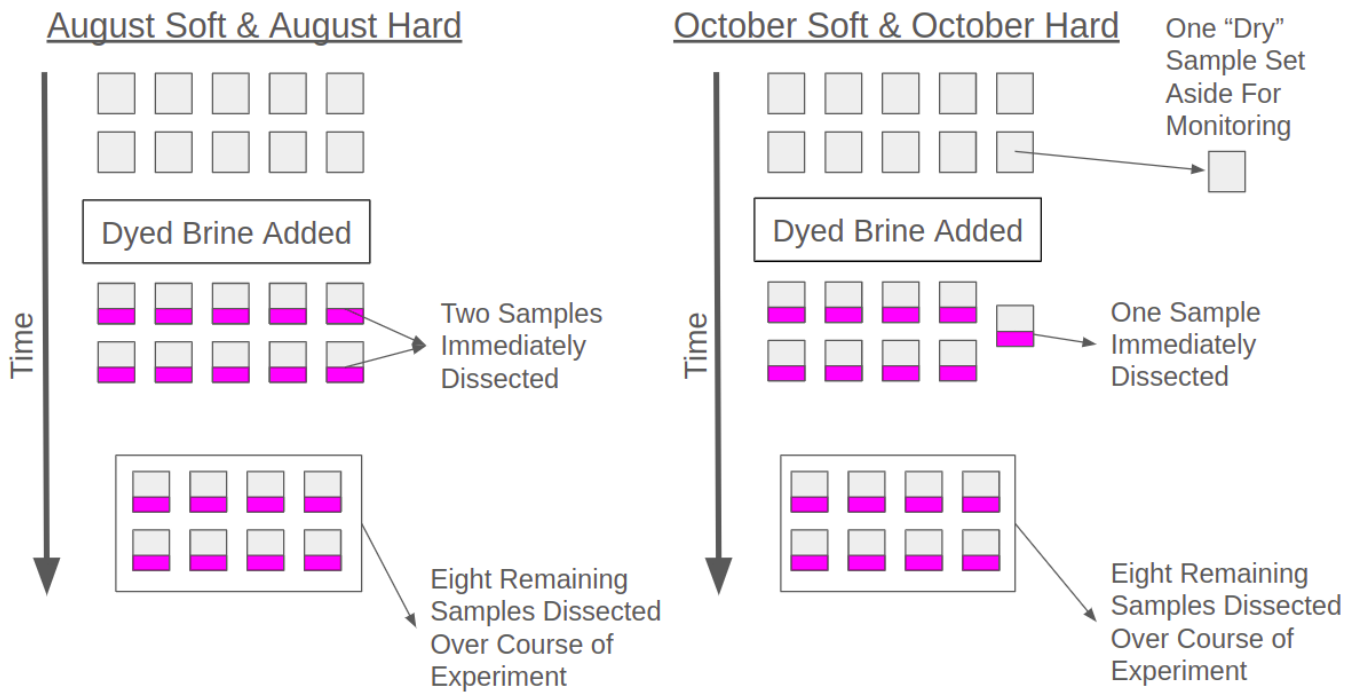


Fig. S4. Schematic of sample allocation strategy. Two dyed samples were immediately dissected in the August experiments. In October, one sample was set aside prior to brine addition so that its rate of settling could be monitored. That left one sample available for immediate dissection, while leaving the same number available for the main experiment.

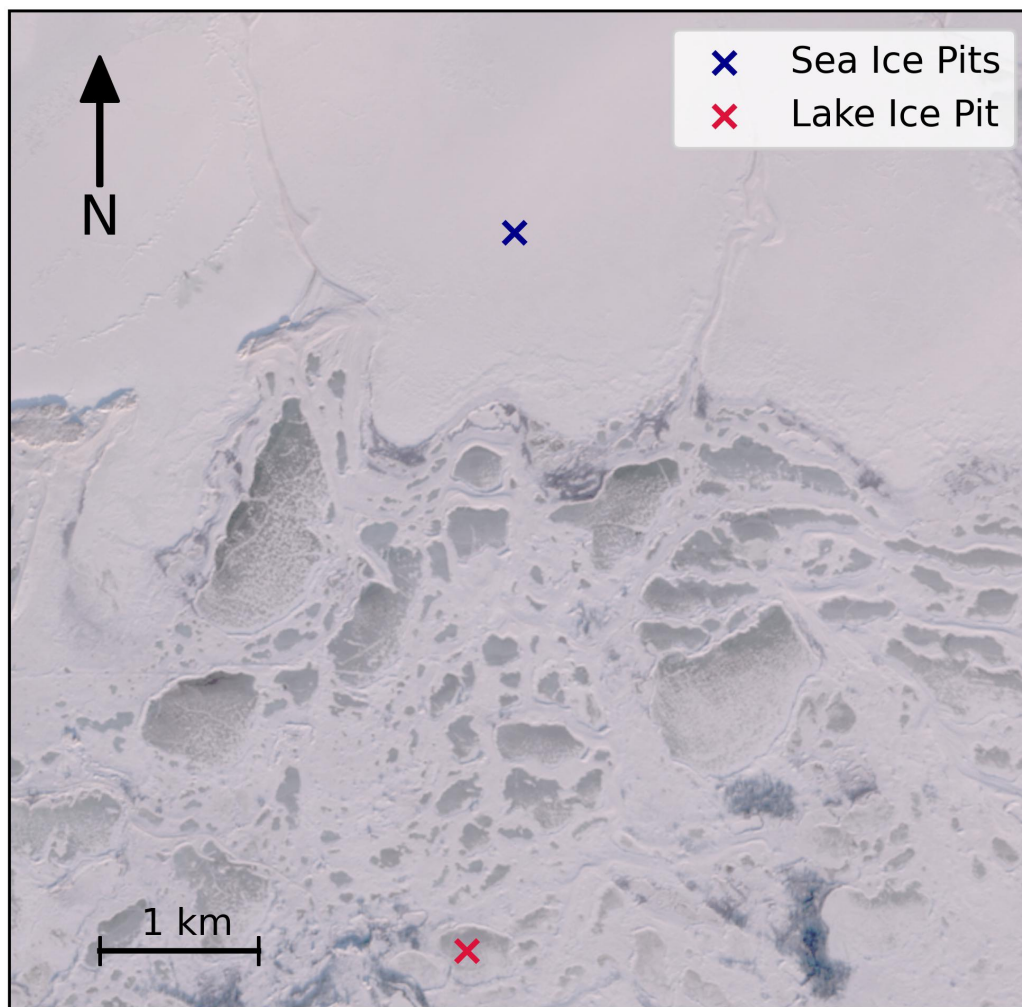


Fig. S5. Locations of the two sites used in the field experiments - blue cross indicates sea ice site on landfast ice, approximately five kilometres to the north of the lake ice site of the control experiment which was adjacent to the Churchill Northern Studies Centre.